

Fast solution of the superconducting dynamo benchmark problem

Leonid Prigozhin¹ and Vladimir Sokolovsky²

¹J. Blaustein Institutes for Desert Research, Ben-Gurion University of the Negev, Sde Boqer Campus 84990, Israel

²Physics Department, Ben-Gurion University of the Negev, Beer-Sheva 84105, Israel

E-mail: leonid@bgu.ac.il and sokolovv@bgu.ac.il.

Abstract

A model of high temperature superconducting dynamo, a promising type of flux pumps capable of wireless injection of a large DC current into a superconducting circuit, has recently been chosen as an applied superconductivity benchmark problem and solved using ten different numerical methods (Ainslie *et al* 2020 *Supercond. Sci. Technol.* **33** 105009). Using expansions in Chebyshev polynomials for approximation in space and the method of lines for integration in time we derive a simple and accurate numerical method which is much faster. The proposed numerical method was applied also to problems with transport current and a field-dependent sheet critical current density.

Keywords: superconducting dynamo, coated conductor, numerical solution, Chebyshev polynomials, singular integral equation

1. Introduction

The high- T_c superconducting (HTS) dynamos are devices capable of inducing a large DC current in a superconducting circuit without the cryogenic losses associated with non-superconducting current leads [1-5]. Mathematical models, explaining the voltage in an HTS strip (the dynamo stator) generated by the dynamo-rotor-attached permanent magnet (PM), have been proposed recently, see [6-10] and the references therein. Available mathematical descriptions are either simplified circuit-type models of the HTS dynamo (e.g. [6]) or consider an infinite superconducting strip subjected to the time-varying non-uniform field of a rotating long PM [7-10]. Models of the latter type are less simplified and better reproduce the non-trivial features of the HTS dynamos.

Such HTS dynamo model, with a coated conductor stator characterized by the nonlinear current-voltage relation with a field-independent critical current density, has been proposed as a new benchmark problem in applied superconductivity and solved by several numerical methods in [11]. These authors computed the generated open-circuit voltage, compared the computation times needed to the methods employed, and made their simulation results available as a supplementary material.

Here we show that an accurate numerical solution of this benchmark problem can be obtained using Chebyshev polynomials for the approximation in space. Resulting semi-discretized problem, a system of ordinary differential equations (ODE), can then be integrated in time using a standard ODE solver with an automatic choice of the time step. Such discretization scheme (the method of lines) helps to control the accuracy of integration. For HTS strips, strip stacks, and pancake coils a similar approach has been proposed in [12]. As in [12], our choice of Chebyshev polynomials for spacial approximation is based on two factors: remarkably fast convergence of the interpolation by Chebyshev polynomial expansions [13] and the ease of using such expansions for solving integral equations with a singular Cauchy-type kernel (see, e.g., [14, 15]). The derived method is much faster than all methods in [11].

Numerical simulations in our work were done using Matlab R2020a on a PC with the Intel (R) Core (TM) i7-9700 CPU@ 3,00 Hz and 32 GB RAM.

2. The benchmark problem

Following [11], we assume that an infinitely long PM with the remanent flux density B_r rotates counter clockwise past a thin stationary HTS strip in the open-circuit configuration (Figure 1); all HTS dynamo parameters are listed in Table 1.

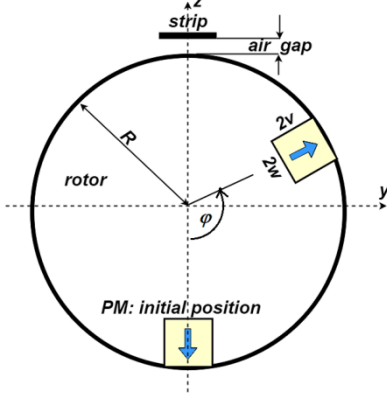


Figure 1. A scheme of an HTS dynamo: the geometry of the benchmark problem.

Table 1. HTS dynamo benchmark parameters (as in [11]).

permanent magnet (PM)	width, $2w$	6 mm
	height, $2v$	12 mm
	active length, l	12.7 mm
	remanent flux density, B_r	1.25 T
HTS stator strip	width, $2a$	12 mm
	thickness	1 μm
	critical current, I_c	283 A
	power value, n	20
rotor external radius, R		35 mm
air gap, d		3.7 mm
frequency of rotation, f		4.25 Hz

If an infinitely long permanent magnet is in the initial position (Figure 1), its magnetic field $\mathbf{H}_0 = (H_{0,y}, H_{0,z})^T$ at a point $\mathbf{p} = (y, z)^T$ outside the magnet is, see [16],

$$H_{0,y}(\mathbf{p}) = -\frac{B_r}{4\pi\mu_0} \left\{ \ln \left[\frac{(y+w)^2 + (\tilde{z}-v)^2}{(y+w)^2 + (\tilde{z}+v)^2} \right] - \ln \left[\frac{(y-w)^2 + (\tilde{z}-v)^2}{(y-w)^2 + (\tilde{z}+v)^2} \right] \right\},$$

$$H_{0,z}(\mathbf{p}) = -\frac{B_r}{2\pi\mu_0} \left\{ \arctan \left[\frac{2v(y+w)}{(y+w)^2 + \tilde{z}^2 - v^2} \right] - \arctan \left[\frac{2v(y-w)}{(y-w)^2 + \tilde{z}^2 - v^2} \right] \right\},$$

where μ_0 is the permeability of vacuum, $\tilde{z} = z + R - v$, R is the rotor radius, $2v$ and $2w$ are the PM height and width, respectively. After rotation of the rotor by an angle φ the field at the point \mathbf{p} becomes

$$\mathbf{H}_{\text{PM}}(\varphi, \mathbf{p}) = A(\varphi)\mathbf{H}_0(A(-\varphi)\mathbf{p}), \quad (1)$$

where

$$A(\varphi) = \begin{pmatrix} \cos \varphi & \sin \varphi \\ -\sin \varphi & \cos \varphi \end{pmatrix}$$

is the matrix of rotation.

Neglecting the strip thickness, we present the strip as $\{-\infty < x < \infty, -a \leq y \leq a, z = z_s\}$, where $2a$ is the strip width, $z_s = R + d$, and d is the air gap. It is assumed the parallel-to-strip electric field component E and the strip sheet current density J are directed along the strip (parallel to the x -axis) and obey the power law,

$$E = E_0 \left| \frac{J}{J_c} \right|^{n-1} \frac{J}{J_c}. \quad (2)$$

Here, as in [11], the field-independent sheet critical current density is $J_c = I_c / 2a$, where I_c is the strip critical current, $E_0 = 10^{-4}$ V/m, the power n is a constant. By the Faraday law, at the strip points $\mathbf{p}_s = (y, z_s)^T$ we have

$$\frac{\partial E}{\partial y} = \mu_0 \frac{\partial H_z}{\partial t}. \quad (3)$$

Here the normal-to-strip component H_z of the total magnetic field is a superposition of the PM and the strip current field components:

$$H_z(t, y) = H_{\text{PM},z}(\varphi(t), \mathbf{p}_s) + \frac{1}{2\pi} \int_{-a}^a \frac{J(t, u)}{y-u} du. \quad (4)$$

Since for all strip points $z = z_s$, to simplify our notations we will omit the dependence on z and write $H_{\text{PM},z}(\varphi(t), y)$ instead of $H_{\text{PM},z}(\varphi(t), \mathbf{p}_s)$. Finally, if a transport current is given, the additional condition is

$$\int_{-a}^a J(t, y) dy = I(t), \quad (5)$$

where $I(t)$ is a known function. The open-circuit condition in the benchmark problem means the transport current I is zero. Jointly with the initial condition $J(0, y) = 0$, equations (1)-(5) fully describe the HTS dynamo benchmark problem [11].

Experimentally, the instantaneous open-circuit voltage at the ends of a stator strip segment has been measured in [2, 7, 9, 10]. Taken for a segment containing the close-to-rotor active zone of the stator, this voltage and its time averaged value are the most important characteristics of an HTS dynamo. In the benchmark model the voltage is suggested to calculate as

$$V(t) = -\frac{l}{2a} \int_{-a}^a E(t, y) dy, \quad (6)$$

where l is the length of the active zone (Table 1).

3. Numerical scheme

Rescaling the variables,

$$J' = J / J_c, \quad (H'_y, H'_z) = (H_y, H_z) / J_c, \quad E' = E / E_0,$$

$$(y', z') = (y, z) / a, \quad t' = \frac{E_0}{\mu_0 J_c a} t, \quad I' = \frac{I}{2aJ_c},$$

omitting the primes, and differentiating equations (4) and (5) with respect to time, we obtain in dimensionless form for $t > 0$, $-1 < y < 1$:

$$E = |J|^{n-1} J, \quad (7)$$

$$\frac{1}{2\pi} \int_{-1}^1 \frac{\dot{J}(t, u)}{y-u} du = \frac{\partial E}{\partial y} - \dot{H}_{\text{PM},z}, \quad (8)$$

$$\int_{-1}^1 \dot{J}(t, y) dy = 2\dot{I}(t). \quad (9)$$

Here the dot above variables means time derivative, the singular integral is understood in the principal value sense.

As in [12], we seek an approximation to the sheet current density in the form of a weighted expansion

$$J(t, y) = \frac{\sum_{i=0}^N \alpha_i(t) T_i(y)}{\sqrt{1-y^2}}, \quad (10)$$

where T_i are Chebyshev polynomials of the first kind and α_i the expansion coefficients. Then we derive a system of ODE for N unknowns, the values $J_k(t) = J(t, y_k)$ in N mesh points, the roots of the Chebyshev polynomial $T_N(y) = \cos[N \arccos(y)]$:

$$y_k = \cos\left(\frac{\pi}{N} \left[k - \frac{1}{2}\right]\right), \quad k = 1, 2, \dots, N. \quad (11)$$

Such meshes are denser near the interval ends and suppress the Runge phenomenon, the instability of polynomial interpolation on uniform meshes [13]. Substituting (10) into equation (8) we use the well-known relation [17]

$$\int_{-1}^1 \frac{T_m(u) du}{(y-u)\sqrt{1-u^2}} = -\pi U_{m-1}(y), \quad (12)$$

where $y \in [-1, 1]$, $U_{m-1}(y) = \sin(m \arccos y) / \sin(\arccos y)$ for $m = 1, 2, \dots$ are Chebyshev polynomials of the second kind, and $U_{-1} = 0$. This yields, for $k = 1, 2, \dots, N$,

$$-\frac{1}{2} \sum_{i=1}^N \dot{\alpha}_i U_{i-1}(y_k) = \left(\frac{\partial E}{\partial y} - \dot{H}_{\text{PM},z} \right) \Big|_{y=y_k}. \quad (13)$$

Substituting (10) also into equation (9) and noting that

$$\int_{-1}^1 \frac{T_m(y) dy}{\sqrt{1-y^2}} = \begin{cases} 0 & m \neq 0 \\ \pi & m = 0 \end{cases},$$

we find $\dot{\alpha}_0 = 2\dot{I}(t) / \pi$. This simple equation ensures the total current constraint (5). Satisfying this constraint using other numerical methods is typically more complicated and needs iterations or adding a penalty term.

Let the J_k values be known at time t . To find the right hand side of equations (13) we calculate the electric field (7) at the mesh nodes, $E_k = |J_k|^{n-1} J_k$, and, approximately, find $\partial E / \partial y$ at the same points by differentiating the Chebyshev expansion interpolating the E_k values (see Appendix A). Furthermore,

$$\dot{H}_{\text{PM},z} = \frac{\partial H_{\text{PM},z}}{\partial \varphi} \frac{d\varphi}{dt} = 2\pi f \frac{\partial H_{\text{PM},z}}{\partial \varphi}.$$

Computing $\partial H_{\text{PM},z} / \partial \varphi$ for $\varphi = \varphi(t)$ at the mesh points y_k (Appendix B), we calculate

$$\psi_k(t) = \left(\partial E / \partial y - \dot{H}_{\text{PM},z} \right) \Big|_{y=y_k}. \quad (14)$$

It is not difficult to construct the expansion ψ in Chebyshev polynomials of the second kind,

$$\psi = \sum_{m=0}^{N-1} \beta_m U_m(y),$$

such that $\psi(y_k) = \psi_k$ (Appendix A). Equations (13) yield then $\dot{\alpha}_i = -2\beta_{i-1}$, $i=1, \dots, N$.

Finally, we set

$$\dot{J}_k(t) = \frac{\sum_{i=0}^N \dot{\alpha}_i(t) T_i(y_k)}{\sqrt{1-y_k^2}}. \quad (15)$$

The ODE system (15) should be integrated in time. In our work we employed a standard Matlab ODE solver, *ode15s*, with the default parameters.

4. Solution of the benchmark problem

To compare our numerical simulation results to those in [11] we return to dimensional variables. As in [11], we assumed zero transport current, simulated ten full rotor rotations, and presented the $V(t)$ curves for the second cycle to avoid the transient dynamics during the first cycle.

First, to estimate the accuracy and convergence rate of our scheme, we solved the problem on different meshes and found that, visually, solutions for $N=100$ and $N=1000$ coincide (Figure 2). The sheet current density evolution during the second cycle is presented in Figure 3.

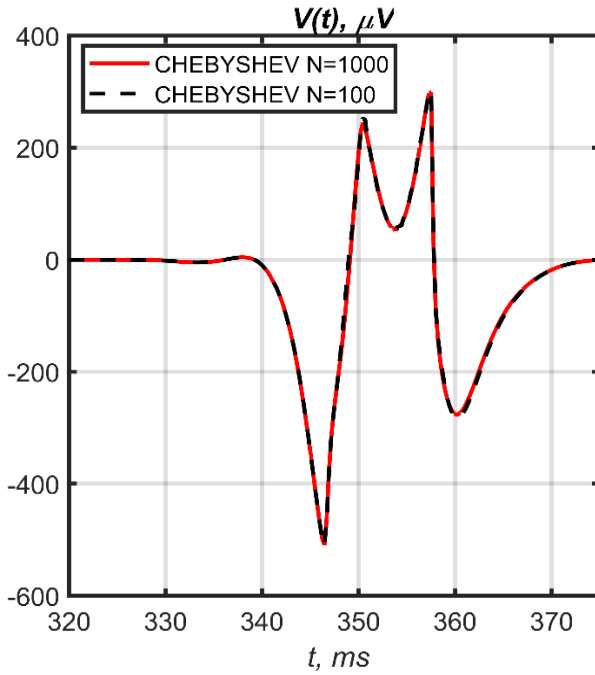


Figure 2. Dynamo generated voltage. Numerical solutions for 100 and 1000 mesh nodes.

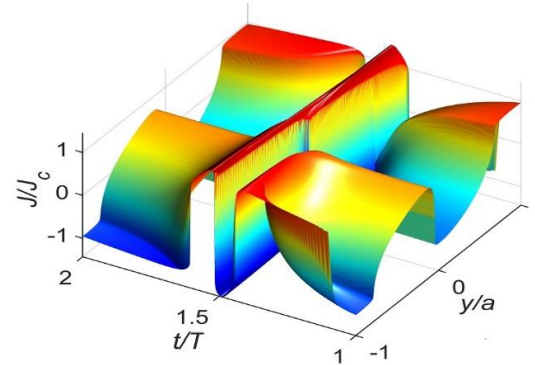


Figure 3. Sheet current density evolution in the second cycle, $T = 1/f$.

Using the supplementary data to [11,18], we found that the $V(t)$ curves obtained using other methods are close. Here (Figure 4) we compare our solution to that of the fastest method in [11], called there MEMEP (the computations by this method have been corrected in [18]). Small differences, observed in this figure near the voltage peaks, are, probably, caused by different approaches to external magnetic field calculation (analytical in our work and numerical in [11]). Ignoring these differences, we can compare convergence of the MEMEP and our method (Table 2).

For this we calculate the L^1 norm, δ^N , of the difference between the voltage $V(t)$ computed with an N -node mesh and that obtained using the same method with the finest mesh (one thousand nodes). For the MEMEP method the necessary data were obtained from [19]. The computation times, presented for similar computers in Table 2, show that similar accuracy can be achieved faster using our method. For other, much slower methods in [11], no accuracy estimates are available.

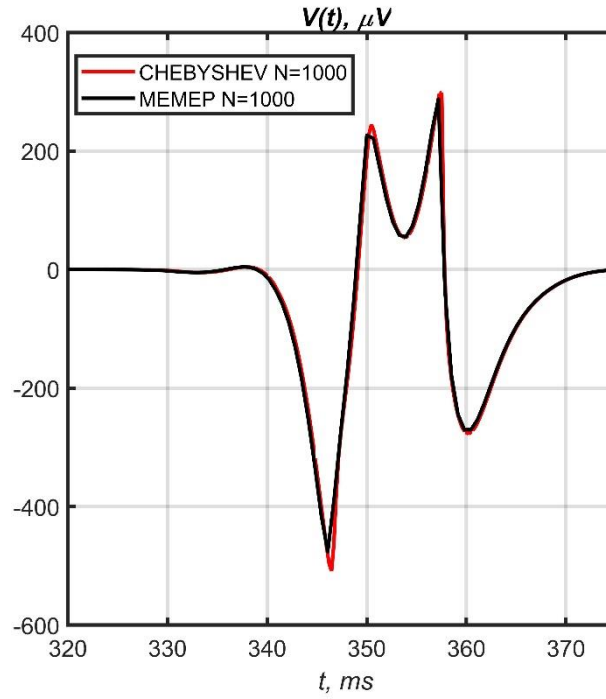


Figure 4. The benchmark problem. Solution by the Chebyshev polynomial-based method versus solution by the fastest finite element method in [11].

Table 2. Convergence of the two methods.

Mesh points, N	Our method		MEMEP	
	CPU time/cycle (s)	Relative error δ^N (%)	CPU time/cycle (s)	Relative error δ^N (%)
100	1.2	2.3	11.5	0.85
200	4.8	0.67	45	0.29
400	33	0.18	155	0.12
1000	612	-	1030	-

5. Extension of the benchmark model

Our method is easily extended to the model with a field-dependent sheet critical current density, e.g.,

$$J_c = \frac{J_{c0}}{1 + h_0^{-1} \sqrt{\kappa H_y^2 + H_z^2}}, \quad (16)$$

Where J_{c0}, h_0, κ are fitting parameters. The parallel-to-film magnetic field component H_y , discontinuous on an infinitely thin film, is usually replaced by the corresponding component of the external field ($H_{PM,y}$ in our case). To compute H_z on each time step, the mesh values $J_k \sqrt{1 - y_k^2}$

are interpolated by the Chebyshev expansion $\sum_{k=0}^{N-1} \alpha_k T_k(y)$ (Appendix A). This presents J in the form (10); substituting (10) into equation (4) and using (12) one obtains

$$H_z(t, y_k) = H_{\text{PM},z}(\varphi(t), y_k) - \frac{1}{2} \sum_{i=1}^{N-1} \alpha_i U_{i-1}(y_k).$$

Finally, the mesh values of J_c are calculated using (16) and the electric field values E_k are determined by the dimensionless form of equation (2).

In our simulations (Figure 5) we chose $J_{c0} = 236$ A/cm equal to the constant J_c in the benchmark problem, $\kappa = 0.5$, and three different values for h_0 . For $h_0 = \infty$ we have $J_c \equiv J_{c0}$ and, the smaller h_0 is, the stronger is the dependence of the sheet critical current density on the magnetic field and the higher is the time-averaged voltage. Qualitatively, the voltage curves in Figure 5 are similar to the experimental ones, see [2, 7, 10].

As a model problem, an HTS dynamo connected to an electronically controlled current supply has been studied, both experimentally and numerically, in [10]. Numerical simulation in that work employed the H -formulation, and so a two-dimensional finite element mesh was needed in the plane orthogonal to the strip; the strip thickness has had to be artificially increased from 1 to 100 μm . A one-dimensional formulation, like the one used in our work, is expected to serve a basis for a more efficient numerical scheme.

Here we solve such a problem for several stator currents (see Figure 6). The field-dependent critical sheet current density (16) with $h_0 = 20J_{c0}$ is assumed; initially, the stator current and the current densities in the strip are zero. The current I was changed linearly with time during the first quarter of the first cycle, then remained a constant fraction of $I_c = 2aJ_{c0} = 283$ A. The mean dynamo generated power is $P = -I \cdot \langle V \rangle$, where $\langle V \rangle$ is the time averaged voltage (see Table 3). Our examples show that, depending on the applied current, this power can be positive (for $I = 0.1I_c$ and $I = -0.2I_c$) or negative (for $I = -0.1I_c$). If the power is positive, the dynamo supplies energy to a load, otherwise the energy is consumed by the dynamo.

For the examples in this Section the computation for $N = 200$ took about six seconds per cycle and, as above, the solutions are shown for the second cycle.

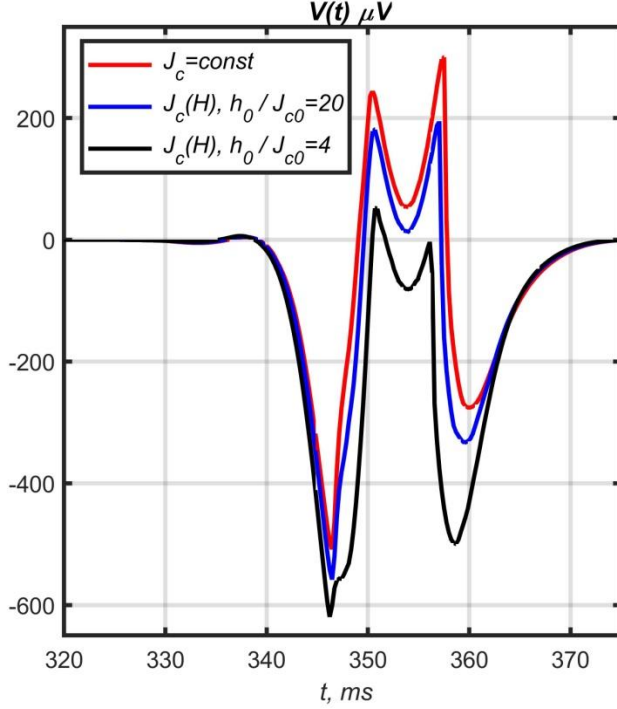


Figure 5. Simulation results for models with field-dependent critical sheet current density.

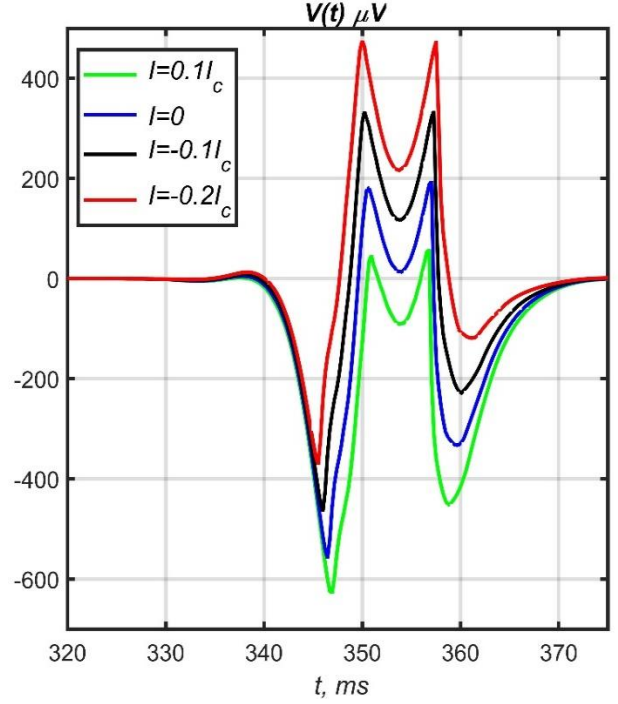


Figure 6. Simulation results for problems with transport current. Here the $J_c(H)$ dependence (16) is employed with $h_0 = 20J_{c0}$.

Table 3. Mean voltage $\langle V \rangle$ during the second cycle for different stator currents.

I / I_c	0.1	0	-0.1	-0.2
$\langle V \rangle, \mu V$	-25.7	-17.8	-5.1	10.8

6. Discussion

Devices for wireless injection of DC supercurrents into closed superconducting circuits open a way to design HTS magnets without thermally inefficient metal current leads. The HTS dynamo considered in our work is a device of this type; the 1D mathematical model [7-10] is able to describe, at least qualitatively, the main features of this device. In [11], this model was chosen as a benchmark problem and solved by a number of numerical methods; a comparison of the efficiency of these methods has been presented. Using expansions in Chebyshev polynomials for approximation in space and the method of lines for integration in time we derived a simple and accurate numerical method which is significantly faster than the methods considered in [11].

Extending the HTS dynamo open circuit benchmark problem, we solved also problems with field-dependent sheet critical current density and problems with transport current. Here we used the most often employed current-voltage dependence given by formulas (2), (16). However, this dependence can be easily replaced by, e.g., interpolation using the experimentally obtained data, as in [7, 8, 10]. Our approach is very efficient also for other superconductivity problems formulated as a singular integral equation of the Cauchy type or a system of such equations [12]. The method can be used also for mathematical modeling the traveling wave flux pumps [20] and multi-PM dynamos [5, 20].

Appendix A. Operations with Chebyshev interpolating expansions

Our numerical scheme makes use of the following linear transformations: (i) from function values at the Chebyshev mesh (11) to coefficients of the interpolating Chebyshev polynomial expansion and vice versa; (ii) from the mesh values of the electric field E to the approximate values of $\partial E / \partial y$ at the same mesh computed as derivatives of the interpolating polynomial; (iii) from the mesh values of E to an approximation of its integral (6). Realization of these operations is described here for completeness.

(i) Let $\mathbf{g} = (g_1, \dots, g_N)^T$ be the vector of function values at the mesh nodes. If $g(y) = \sum_{i=1}^N \gamma_i T_{i-1}(y)$ is the interpolating expansion in Chebyshev polynomials of the first kind, then $A\mathbf{y} = \mathbf{g}$, where the i -th column of the $N \times N$ matrix A is the vector $(T_{i-1}(y_1), \dots, T_{i-1}(y_N))^T$. Efficient calculation of this matrix is based on the recurrent relation: $T_0 = 1$, $T_1 = y$, and $T_k = 2yT_{k-1} - T_{k-2}$ for $k \geq 2$. Multiplication by this matrix realizes transition from the expansion coefficients to function values; the inverse matrix is used for transition from function values to the expansion coefficients. Similarly, interpolation by the expansion in Chebyshev polynomials of the second kind, $g(y) = \sum_{i=1}^N \delta_i U_{i-1}(y)$, is related to the matrix B with the i -th column $(U_{i-1}(y_1), \dots, U_{i-1}(y_N))^T$; the matrix calculation is based on the relations: $U_0 = 1$, $U_1 = 2y$, and $U_k = 2yU_{k-1} - U_{k-2}$ for $k \geq 2$.

(ii) For a given vector \mathbf{E} of $E_k = E(t, y_k)$ values, the derivatives $E'_k = \partial E / \partial y|_{t, y_k}$, see (14), are approximated by derivatives of the interpolating expansion $E = \sum_{i=1}^N \gamma_i T_{i-1}(y)$ with $\boldsymbol{\gamma} = A^{-1} \mathbf{E}$. Since $dT_k / dy = kU_{k-1}$, we have $E' = \sum_{i=2}^N (i-1)\gamma_i U_{i-2}(y)$. Let C be the $N \times N$ matrix with elements

$$C_{ij} = \begin{cases} i & j = i+1 \\ 0 & j \neq i+1 \end{cases}.$$

Then $E' = BC\boldsymbol{\gamma} = DE$, where the $N \times N$ differentiation matrix $D = BCA^{-1}$.

(iii) Denote, for $i = 0, \dots, N-1$,

$$\sigma_{i+1} = \int_{-1}^1 T_i(y) dy = \begin{cases} \frac{2}{1-i^2} & i \text{ is even,} \\ 0 & i \text{ is odd.} \end{cases}$$

For $E = \sum_{i=1}^N \gamma_i T_{i-1}(y)$ we obtain $\int_{-1}^1 E dy = \boldsymbol{\gamma}^T \cdot \boldsymbol{\sigma} = (A^{-1} \mathbf{E})^T \cdot \boldsymbol{\sigma} = \mathbf{E}^T \cdot (\boldsymbol{\sigma}^T A^{-1})^T = \mathbf{E}^T \cdot \boldsymbol{\eta}$, where $\boldsymbol{\sigma} = (\sigma_1, \dots, \sigma_N)^T$ and $\boldsymbol{\eta} = (\boldsymbol{\sigma}^T A^{-1})^T$.

We note that matrices A, A^{-1}, B, B^{-1}, D are used on each time step but, as well as the vector $\boldsymbol{\eta}$, should be calculated only once. For, e.g., $N = 200$ this takes about 0.01 second and ensures the efficiency of our simulations.

Appendix B. Computing $\partial H_{\text{PM},z} / \partial \varphi$: interpolation from a lookup table

We define a uniform mesh with $(N_\varphi + 1)$ nodes φ_i in $[0, 2\pi]$ and find H_{PM} analytically at the strip grid points y_1, \dots, y_N for every PM rotation angle φ_i using (1). The lookup tables of $H_{\text{PM},y}(\varphi_i, y_k)$

and $H_{PM,z}(\varphi, y_k)$ are needed if the critical current density depends on magnetic field. The normal to strip component $H_{PM,z}(\varphi, y_k)$ is, for each y_k , a periodic function of φ sampled at the angles φ_i and $\partial H_{PM,z}(\varphi_i, y_k)/\partial\varphi$ values were obtained by numerical differentiation in the Fourier space using the fast Fourier transform. In our simulations we chose $N_\varphi = 2^{12}$; for $N = 200$ computing these tables takes about 0.1 second. Linear interpolation from the lookup tables provides a fast and accurate approximation to $H_{PM,y}(\varphi, y_k)$, $H_{PM,z}(\varphi, y_k)$, and $\partial H_{PM,z}(\varphi, y_k)/\partial\varphi$ for any rotation angle $\varphi(t)$.

ORCID iD

Leonid Prigozhin <https://orcid.org/0000-0002-2448-4471>
 Vladimir Sokolovsky <https://orcid.org/0000-0003-4887-413X>

References

- [1] Hoffmann C, Pooke D, and Caplin A D 2011 Flux pump for HTS magnets *IEEE Trans. Appl. Supercond.* **21** 1628-31
- [2] Bumby C W, Jiang Z, Storey J G, Pantoja A E and Badcock R A 2016 Anomalous open-circuit voltage from a high- T_c superconducting dynamo *Appl. Phys. Lett.* **108** 122601
- [3] Hamilton K, Mataira R, Geng J, Bumby C, Carnegie D and Badcock R 2020 Practical estimation of HTS dynamo losses *IEEE Trans. Appl. Supercond.* **30** 4703105
- [4] Ma J, Geng J, Gawith J, Zhang H, Li C, Shen B, *et al.* 2019 Rotating permanent magnets based flux pump for HTS no-insulation coil *IEEE Trans. Appl. Supercond.* **29** 5202106
- [5] Storey J G, Pantoja A E, Jiang Z, Badcock R A and Bumby C W 2019 Optimizing rotor speed and geometry for an externally mounted HTS dynamo *IEEE Trans. Appl. Supercond.* **29** 5202705
- [6] Campbell A 2019 A circuit analysis of a flux pump *Supercond. Sci. Technol.* **32** 115009
- [7] Mataira R C, Ainslie M D, Badcock R A and Bumby C W 2019 Origin of the DC output voltage from a high- T_c superconducting dynamo *Appl. Phys. Lett.* **114** 162601
- [8] Ghabeli A and Pardo E 2020 Modeling of airgap influence on DC voltage generation in a dynamo-type flux pump *Supercond. Sci. Technol.* **33** 035008
- [9] Mataira R, Ainslie M D, Badcock R and Bumby C W 2020 Modeling of stator versus magnet width effects in high- T_c superconducting dynamos *IEEE Trans. Appl. Supercond.* **30** 5204406
- [10] Mataira R, Ainslie M, Pantoja A, Badcock R and Bumby C 2020 Mechanism of the high- T_c superconducting dynamo: Models and experiment *Phys. Rev. Appl.* **14** 024012
- [11] Ainslie M, Grilli F, Quéval L, Pardo E, Perez-Mendez F, Mataira R, *et al.* 2020 A new benchmark problem for electromagnetic modelling of superconductors: the high- T_c superconducting dynamo *Supercond. Sci. Technol.* **33** 105009
- [12] Sokolovsky V, Prigozhin L and Kozyrev A B 2020 Chebyshev spectral method for superconductivity problems *Supercond. Sci. Technol.* **33** 085008
- [13] Trefethen L N 2013 *Approximation theory and approximation practice* (Philadelphia, PA: Siam)
- [14] Eshkuvatov Z, Long N N and Abdulkawi M 2009 Approximate solution of singular integral equations of the first kind with Cauchy kernel *Appl. Math. Lett.* **22** 651-7
- [15] Mondal S and Mandal B 2019 Solution of singular Integral equations of the first kind with Cauchy kernel *Comm. Adv. Math. Sci.* **2** 69-74
- [16] Furlani E P 2001 *Permanent magnet and electromechanical devices: materials, analysis, and applications* (San Diego, CA: Academic Press)
- [17] Mason J C and Handscomb D C 2002 *Chebyshev polynomials* (Boca Raton, FL: CRC press)
- [18] Ainslie M, Grilli F, Quéval L, Pardo E, Perez-Mendez F, Mataira R, *et al.* 2021 Corrigendum: A new benchmark problem for electromagnetic modelling of superconductors: the high- T_c superconducting dynamo *Supercond. Sci. Technol.* **34** 029502

- [19] A. Ghabeli, private communication, 2021
- [20] Zhai Y, Tan Z, Liu X, Shen B, Coombs T A and Wang F 2020 Research Progress of Contactless Magnetization Technology: HTS Flux Pumps *IEEE Trans. Appl. Supercond.* **30** 4602905